Many-body formulation of carriers capture time in Quantum Dots applicable to device simulation codes

Many-body formulation of carriers capture time in quantum dots applicable in device simulation codes

Marco Vallone[a)]
Dipartimento di Elettronica, Politecnico di Torino, Torino 10126, Italy

(Received 28 January 2009; accepted 14 January 2010; published online 11 March 2010)

We present an application of Green's functions formalism to calculate in a simplified but rigorous way electrons and holes capture time in quantum dots in closed form as function of carrier density, levels confinement potential, and temperature. Carrier-carrier (Auger) scattering and single LO-phonon emission are both addressed accounting for dynamic effects of the potential screening in the single plasmon pole approximation of the dielectric function. Regarding the LO-phonons interaction, the formulation evidences the role of the dynamic screening from wetting-layer carriers in comparison with its static limit, describes the interplay between screening and Fermi band filling, and offers simple expressions for capture time, suitable for modeling implementation. © *2010 American Institute of Physics*. [doi:10.1063/1.3309838]

I. INTRODUCTION

Semiconductor lasers and optical amplifiers using quantum dots (QDs) are very promising devices due to their potential in ultrafast optical communications.[1] Self-assembled QD is typically grown on quasi-two-dimensional wetting layer[2] (WL) and gain dynamics is governed by capture of carriers from WL in the QDs levels as well as by their relaxation between the discrete QD states,[3–5] so a quantitative description of various electronic scattering processes is necessary.

Electrons and holes dynamics in semiconductor nanostructures has been extensively studied in literature.[6] Many works have shown that, in III–V semiconductor heterostructures, capture and relaxation processes mainly happen through carrier-carrier (Auger) scattering and LO-phonons emission.[7–9] Generally, other mechanisms besides these exist and contribute to the total capture and relaxation, but especially for high carrier density, Auger scattering provide the dominant relaxation channel. Energy separation of QD states typically does not match the LO-phonon energy and also the electrons QD confinement energy often exceeds it, preventing electrons capture via LO-phonons emission. Holes instead have more shallow confinement energy than electrons and this channel may be very effective when carrier density is low.[10]

A full understanding of how these characteristic times vary with carrier density, temperature, and confinement energies has consequently great importance in development of rate equation models for such devices.[11] Many works in literature address the carrier capture in a very complete fashion, often describing in detail and taking into account a huge number of different contributions,[10] but without giving the reader simple formulae able to present the problem solution in a way ready to be converted in fast software routines.

When capture and relaxation times are needed for many density values (e.g., if their calculation have to be used in a modeling activity) or if an easy understanding of underlying device physics is desired, a bit simplified, but still self-consistent formulation, able to drive design guidelines may be useful. In this paper we present a derivation of the electrons and holes capture rates in QD through Auger scattering with WL carriers and LO-phonon emission, exploiting as much as possible analytic techniques, in order to end with explicit formulations, giving maximum evidence of the role of carrier density, temperature, and QD level energy confinement with respect to WL. The price to pay will be to find out the best tradeoff between completeness and simplification. We stress that simplified but explicit expressions of capture time as function of WL carrier density are not available in literature in the present form, nor a direct comparison between results obtained using static and dynamic expressions of the LO-phonon screening.

Screening of the Coulomb interaction is treated in this paper using full dynamic, single plasmon pole (SPP) expression of the random phase approximation (RPA) dielectric function[12] for both the scattering mechanisms addressed here, avoiding the use of the full RPA formulation probably addressable only with numerical techniques. The semianalytic expressions that we obtained enables us to distinguish easily between Fermi-blocking effects due to band filling and screening of the interaction, studying them separately, if desired, or evaluating their mutual interplay.

It has been avoided to link this model to any particular expressions of QD and WL wave functions, but clearly indicating how to deal with them. It is the scope of the paper (a) to introduce a formal, nonapproximate expression of carrier capture time in a WL-QD system in the presence of plasma, (b) to show that the computational effort involved in standard calculations can be much reduced by using our expressions, and (c) to validate our approach reproducing example of results normally obtained by much more heavy calculations.

In Sec. II we summarize the general theory of the capture and relaxation rate in a Green's function based formalism, valid at finite temperature, including both Auger and

[a)]Electronic mail: marco.vallone@polito.it.

single LO-phonon scattering processes. In Sec. III we find complete, general expression of the carrier capture rate, including (but keeping separated) both scattering processes, investigating the role of the coupled phonon-plasmon system. Then, in Sec. IV, a simplified but analytic expression in the Thomas–Fermi static limit is derived for LO-phonon contribution, in order to compare it with the more general dynamic formulation. In Sec. V plots of capture time coming from these two channels are given as a function of carrier density and level confinement, illustrating the interplay of the two mechanisms. The paper will end with a brief discussion on the main results, advantages and limitations of this model, then in Sec. VI conclusions have been drawn.

II. GENERAL THEORY

The energy broadening of an electron (hole) state characterized by in-plane wave vector $\vec{k}$ in the i-subband, due to the Auger and LO-phonon interactions, is described by the spectral function $A_i(\vec{k},\omega)$. This is related to the retarded Green's function for the interacting electron by the relation $A_i(\vec{k},\omega)=-2\ \mathrm{Im}[G_{ii}(\vec{k},\omega)]$, being the dressed Green's function $G_{ii}(\vec{k},\omega)$ determined by the Dyson equation,[12]

$$G_{ij}=G_l^0\delta_{ij}+G_l^0\sum_m \Sigma_{lm}(\vec{k},\mathrm{i}p_m)G_{mj} \tag{1}$$

("Im" means the imaginary part as usual. In the entire document, the italic "i" is an index, whereas normal "i" is the imaginary unit). In Eq. (1) the retarded self-energy $\Sigma_{lm}(\vec{k},\mathrm{i}p_m)$ can be evaluated at various levels of approximation; the simplest one is given by

$$\Sigma_{lm}(\vec{k},\mathrm{i}p_m)=-\frac{1}{\beta}\sum_{\mathbf{q},\omega_n,j} V_{jlmj}^{\mathrm{eff}}(q,\mathrm{i}\omega_n)G_{jj}^0(\vec{k}-\vec{q},\mathrm{i}p_m+\mathrm{i}\omega_n). \tag{2}$$

Here β is the inverse temperature in energy units, $\mathrm{i}p_m$ and $\mathrm{i}\omega_n$ are the standard Fermi and Bose imaginary frequencies, as introduced in the Matsubara's formalism.[12] The noninteracting, diagonal quasiequilibrium electron Green's function in the jth subband is given by

$$G_{jj}^0(\vec{k}-\vec{q},\mathrm{i}p_m+\mathrm{i}\omega_n)=\frac{1}{\hbar}\frac{n_{\mathrm{WL}}(k)}{(\mathrm{i}p_m+\mathrm{i}\omega_n-\Delta\omega_j)}, \tag{3}$$

where $\hbar$ is the reduced Planck's constant, $-\hbar\Delta\omega_j=\hbar^2|\vec{k}-\vec{q}|^2/(2m)+E_j$, and $n_{\mathrm{WL}}(k)$ is the Fermi distribution for the WL in-plane $\vec{k}$ state. Here E_j is the energy of the j-subband and m is the carrier effective mass.

The next level of approximation is known as the *self-consistent* one,[13] in which the dressed electron Green's function is used in Eq. (2) instead of the simpler noninteracting one. In both cases self-energy has real and imaginary parts, but in the latter case vertex corrections are self-consistently taken into account within the scattering process. It is customary[12,14,15] in modeling devoted applications to do not follow such a complicated path, assuming the expression in Eq. (2) as enough accurate approximation of the real situation. Actually, the aim of this paper is to illustrate a fast and applications devoted method of capture-rate calculation, based on Green's function approach. The simplification introduced making use in Eq. (2) of the undressed Green's function is not an oversimplification. As a matter of fact, many-body effects effectively enter in the equations through the screened interaction and this is, for example, the approach followed in Ref. 15. If corrections introduced using the dressed Green's function is small compared to the energy separation between subbands, this is a valid approximation. If this was not verified, a better degree of approximation would consist in introducing in Eq. (2) a renormalization term, treating it as in Ref. 16. The resulting equations resulted unchanged, except for the self-energy correction to E_0 wherever it appears. Good examples of another approach, based on Coulomb scattering matrix formalism, are represented by Refs. 17 and 18.

If only diagonal terms of the self-energy are retained in the scattering rate calculation from j-th to m-th subband (a valid hypothesis if nondiagonal terms are small compared with energy separation within subbands, see Ref. 14), retarded self-energy simply reads as

$$\Sigma_{mm}(\vec{k},\mathrm{i}p_m)=-\frac{1}{\beta\hbar}\sum_{\vec{q}}\sum_n V^{\mathrm{eff}}(q,\mathrm{i}\omega_n)\frac{n_{\mathrm{WL}}(k)}{\mathrm{i}p_m+\mathrm{i}\omega_n-\Delta\omega_j}. \tag{4}$$

Spectral function is a Lorentzian centered near Green's function pole, whose half-width at half-height is given by imaginary part of $\Sigma_{mm}(\vec{k},\mathrm{i}p_m)$ and capture rate $\tau_{\vec{k}j\to m}^{-1}$ is given by

$$\tau_{\vec{k}j\to m}^{-1}=-\frac{2}{\hbar}\mathrm{Im}\ \Sigma_{mm}(\vec{k},\mathrm{i}p_m). \tag{5}$$

In Eq. (4), effective potential for the coupled carrier-carrier and carrier-LO-phonon interactions in the WL takes the form[12]

$$V^{\mathrm{eff}}(q,\omega)=\frac{V_0(q)}{\varepsilon_\infty\varepsilon(q,\omega)}-\frac{M_q^2}{\varepsilon(q,\omega)^2}D(q,\omega). \tag{6}$$

Here

$$V_0(q)=\frac{2\pi e^2}{q}F_{j,m}(q), \tag{7}$$

whereas $\varepsilon(q,\omega)=1-[V_0(q)/\varepsilon_\infty]P(q,\omega)$ is the carrier-carrier part of the screened dielectric function.

$M_q^2=(1/\varepsilon_\infty-1/\varepsilon_0)\omega_{\mathrm{LO}}V_0(q)$ is the unscreened carrier-phonon matrix element and

$$D(q,\omega)=\frac{\omega_{\mathrm{LO}}}{\omega^2-\omega_{\mathrm{LO}}^2-\dfrac{M_q^2}{\varepsilon(q,\omega)}\omega_{\mathrm{LO}}P(q,\omega)} \tag{8}$$

is the phonon renormalized Green's function. The form factor $F_{j,m}(q)$ depends on the explicit form of the initial and final states eigenfunctions (see below).

We assume dispersionless bulk LO-phonons and single-oscillator model in which the LO-phonon frequency ω_{LO}, the TO-phonon frequency ω_{TO}, the static (ε_0), and optical (ε_∞) constants are related by the Lyddane–Sachs–Teller[19] relationship $(\omega_{\mathrm{LO}}/\omega_{\mathrm{TO}})^2=\varepsilon_0/\varepsilon_\infty$. A rigorous derivation of the total dielectric function would show that electron-phonon and

electron–electron scattering contributions affect each other in a very complicated way. In a diagrammatic calculation of the polarization $P(q,\omega)$ of the electron gas, diagrams in which the basic electron bubble has internal phonon lines would represent this, but for practical purposes the RPA approximation is accurate enough.

Treating contributions to the dielectric function as simply additive, *screened* electron-electron interactions and *screened* electron-phonon interactions are treated on equal footing and both contributions may be summed and considered simultaneously at play.

The Green's function in Eq. (4) describes an electron (hole) scattering from a state of momentum $\vec{k}$ in the j-th WL subband into a state of momentum in $\vec{k}-\vec{q}$ the mth QD subband, by phonon emission or by Auger scattering. In this formulation and looking at Eq. (5), the two contributions to scattering rate are well evident, the former representing Auger scattering, the latter representing the screened carrier-phonon interaction.

The $F_{j,m}(q)$ form factor for the coupled WL-QD is given by

$$F_{j,m}(q) = \int_{-\infty}^{\infty}\int_{-\infty}^{\infty} \Psi^*_{m,\mathrm{QD}}(q,z_1)\Psi^*_{j,\mathrm{QW}}(q,z_2) \times \exp(-q|z_1-z_2|) \times \Psi_{m,\mathrm{QD}}(q,z_1)\times\Psi_{j,\mathrm{QW}}(q,z_2)dz_1\ dz_2, \tag{9}$$

where $\Psi_{\mathrm{QW}}(q,z)$ and $\Psi_{\mathrm{QD}}(q,z)$ are unity-normalized z-envelope wave function (being z the epitaxial growth direction). In the limit $q|z_1-z_2| \ll 1$ we may discard the exponential. If wave functions do not depend much on q, $F_{i,m}(q)$ can be approximated with the superposition integral

$$I_{j,m} = \int_{-\infty}^{\infty}\int_{-\infty}^{\infty} \Psi^*_{m,\mathrm{QD}}(z_1)\Psi^*_{j,\mathrm{QW}}(z_2)\Psi_{m,\mathrm{QD}}(z_1) \times\Psi_{j,\mathrm{QW}}(z_2)dz_1\ dz_2, \tag{10}$$

not depending on q. Strain effects and confinement are obviously included in their profile and will not be addressed here (they may be computed in many convenient ways, e.g., see Ref. 20). We stress that this simplification is not necessary and expression given by Eq. (9) may be easily put in the model, for example in cases of pyramidal-shape QD, for which wave functions cannot be factorized in a z-dependent and an in-plane-dependent factors. Nevertheless Eq. (10) may be used as an acceptable approximation to better understand the main underlying physics.

In this context, capture rates are given by

$$\tau^{-1}_{kj\to m} = \frac{2}{\beta\hbar^2}\mathrm{Im}\left[\sum_{\vec{q}}\sum_{n}\frac{V^{\mathrm{eff}}(q,i\omega_n)n_{\mathrm{WL}}(k)}{ip_m+i\omega_n-\Delta\omega_j}\right], \tag{11}$$

in which Eqs. (6)–(9) and eventually Eq. (10) are to be used and are intended as the in-scattering rate from WL to the mth level of QD (see e.g., Ref. 10). Let us now separately investigate the two capture mechanisms.

III. CAPTURE VIA AUGER SCATTERING

The carrier-carrier interaction is described by the first term of the right hand side of Eq. (6), in which we employ the dynamic expression of the dielectric constant in the SPP approximation, retaining also the so-called Lundquist term, whose inverse is given by

$$\frac{1}{\varepsilon_\infty\varepsilon(q,\omega)} = \frac{1}{\varepsilon_\infty}\left(1+\frac{\Omega_q^2}{\omega^2-\omega_q^2}\right), \tag{12}$$

where $\Omega_q = \sqrt{2\pi e^2 Nq/\varepsilon_0\mu}$ is the WL two-dimensional (2D), q-dependent plasma frequency,[12] N is the 2D WL particle density and μ is the electron-hole reduced effective mass. The quantity

$$\omega_q = \sqrt{\Omega_q^2(1+q/\kappa)+Cq^4} \tag{13}$$

is the so called *effective plasmon frequency*, in which κ is the N-dependent screening wave vector and C is a numerical constant.[21]

Now, we will follow the classical way to manage frequency summation, generalizing for this case the method shown in Ref. 12, the Matsubara's frequency summation. It may be demonstrated that, converting the n-summation into an integral and extending it to the complex plane with $z=i\omega_n$, a summation $\Sigma_n f(\omega_n)$ over Bose frequencies is given by $-\hbar\beta\Sigma_{z_i} f(z_i)n_B(z_i)$, where $n_B(z_i)$ is the Bose–Einstein distribution and summation runs over residues of $f(z)$ in the complex plane. Assuming that capture happens into a QD level having energy E_0 below the ground state WL level (confinement energy), lengthy but direct calculation gives the following capture rate expression due to Auger scattering of WL carriers having momentum $\vec{k}$ with electrons or holes in the same WL subband (normally conduction band WL has one subband only and we assume it as true),

$$\tau^{-1}_{kj\to m} = \frac{2\pi^2e^2}{\hbar\varepsilon_\infty}n_{\mathrm{WL}}(k)\mathrm{Im}\sum_q\frac{F_{j,m}(q)}{q}\frac{\Omega_q^2}{\omega_q} \times\frac{1+n_B(\hbar\omega_q)-n_F(\hbar\Delta\omega_j)}{\omega_q+\Delta\omega_j-i\eta}. \tag{14}$$

Rates due to e-e or e-h scattering are additive and may be obtained by using each time the correct effective masses in Eqs. (12)–(14). Converting summation into a 2D integral according to $\Sigma_q R(q) = 2/(2\pi)^3\int_0^{2\pi}\int_0^{\infty}R(q)q\ dq\ d\vartheta$, provided translational invariance is fulfilled (the 2 is for WL spin states summation), we obtain

$$\tau^{-1}_{kj\to m} = \frac{\alpha cm}{\pi^2\hbar\varepsilon_\infty}n_{\mathrm{WL}}(k)\mathrm{Im}\int_0^{2\pi}d\vartheta\int_0^{\infty}dq\ F_{j,m}(q)\frac{\Omega_q^2}{\omega_q} \times\frac{1+n_B(\hbar\omega_q)-n_F(\hbar\Delta\omega_j)}{-q^2-k^2+2kq\cos(\theta)+\frac{2m(\hbar\omega_q-E_0)}{\hbar^2}-i\eta}, \tag{15}$$

in which m is the effective mass of the captured carrier, n_F is the Fermi distribution, α is the fine structure constant, and c is the speed of light in vacuum, whereas the positive infinitesimal η accounts for Green's function causality prescrip-

tion. Exploiting the following identity in order to integrate over angle:

$$\int_0^{2\pi} \frac{d\vartheta}{a - b\cos(\theta)} = \frac{2\pi}{\sqrt{a^2 - b^2}}, \tag{16}$$

we get rid of ϑ integration,

$$\tau_{kj\to m}^{-1} = \frac{2\alpha c m}{\pi\hbar\varepsilon_\infty} n_{\mathrm{WL}}(k) \times \mathrm{Im}\int_0^\infty dq \times \frac{F_{j,m}(q)\dfrac{\Omega_q^2}{\omega_q}[1 + n_B - n_F]}{\sqrt{\left[\dfrac{2m(\hbar\omega_q - E_0)}{\hbar^2} - q^2 - k^2 - \mathrm{i}\eta\right]^2 - 4k^2q^2}}, \tag{17}$$

having averaged the weak θ-dependence in argument of n_F.

This expression may be numerically evaluated without any difficulty, averaging over a thermalized distribution of k-states in the WL plane. A more simplified expression of Eq. (17) may also be given, valid for carriers with $\vec{k}=0$,

$$\tau_{0j\to m}^{-1} = \frac{2\alpha c m}{\pi\hbar\varepsilon_\infty} n_{\mathrm{WL}}(k)\mathrm{Im}\int_0^\infty F_{j,m}(q) \times \frac{\dfrac{\Omega_q^2}{\omega_q}(1 + n_B - n_F|_{k=0})}{\dfrac{2m(\hbar\omega_q - E_0)}{\hbar^2} - q^2 - \mathrm{i}\eta} dq. \tag{18}$$

IV. CAPTURE VIA PHONON EMISSION

The electron-phonon interaction is described by the second term of the right hand side of Eq. (6), in which we employ again the full dynamic expression of the dielectric constant in the SPP approximation. With these expressions, self-energy assumes the form

$$\Sigma_{mm}(\vec{k}, ip_m) = \frac{1}{\hbar\beta} \times \sum_{q,n} F_{j,m}(q)\frac{M_q^2 D(q,\omega_n)}{\varepsilon_\infty{}^2\varepsilon(q,\omega)^2}\frac{n_{\mathrm{WL}}(k)}{ip_m + \mathrm{i}\omega_n - \Delta\omega_j}, \tag{19}$$

in which the dielectric constant shown in Eq. (12) has to be used. In order to execute frequency summation, we have to study the form of the summand $M_q^2 D(q,\omega)/\varepsilon(q,\omega)^2$. It has poles at frequencies ω_+, ω_-, and ω_q, where

$$\omega_\pm^2 = \frac{1}{2}(\omega_q^2 + \omega_{\mathrm{LO}}^2) \pm \frac{1}{2}\sqrt{(\omega_{\mathrm{LO}}^2 - \omega_q^2)^2 + 4\left(\frac{1}{\varepsilon_\infty} - \frac{1}{\varepsilon_0}\right)\Omega_q^2\omega_{\mathrm{LO}}^2}. \tag{20}$$

It is noticeable that this quadratic form recovers the well-known plasmon frequency expression if q tends to zero.[21]

With the given expression of the full-dynamic dielectric constant, Eq. (19) becomes

$$\Sigma_{mm}(\vec{k}, ip_m) = \frac{K_\varepsilon\omega_{\mathrm{LO}}^2}{\hbar\beta}\sum_{q=0}^{\infty}\frac{2\pi e^2 F_{j,m}(q)}{\varepsilon_\infty(q)} \times \sum_{n=-\infty}^{\infty}\frac{(\omega_n^2 + \Omega_q^2 - \omega_q^2)^2}{(\omega_n^2 - \omega_+^2)(\omega_n^2 - \omega_-^2)(\omega_n^2 - \omega_q^2)} \times \frac{n_{\mathrm{WL}}(k)}{ip_m + \mathrm{i}\omega_n - \Delta\omega_j} \tag{21}$$

having defined $K_\varepsilon = (\varepsilon_\infty^{-1} - \varepsilon_0^{-1})$.

Now, we will follow again the classical way to manage frequency summation, generalizing the Matsubara's frequency summation method for this more complicated case. First of all, we form the triple of plasma modes $(\omega_+ \ \omega_- \ \omega_q)$ and indicate it as $(\omega_1 \ \omega_2 \ \omega_3)$. We convert the n-summation into an integral and extend it to the complex plane, exploiting the residual calculation theorems. Lengthy but direct calculation gives the following capture rate expression, having converted the q-summation into an integral over q:

$$\tau_{\vec{k}j\to m}^{-1} = \frac{\alpha c K_\varepsilon\omega_{\mathrm{LO}}^2 n_{\mathrm{WL}}(k)}{\pi^2}\mathrm{Im}\int_0^\infty\int_0^{2\pi} F_{j,m}(q)\{S_{123}(k,q) + S_{312}(k,q) + S_{231}(k,q) - G(k,q)\}d\vartheta\ dq, \tag{22}$$

where

$$S_{lmn}(k,q) = -\frac{(\omega_l^2 + \Omega_q^2 - \omega_q^2)^2}{2\omega_l(\omega_l^2 - \omega_m^2)(\omega_l^2 - \omega_n^2)(\Delta\omega_j - \omega_l)} \times \left(1 + \frac{2\omega_l}{(\Delta\omega_j + \omega_l)}n_B(\hbar\omega_l)\right) \tag{23}$$

and

$$G(k,q) = -\frac{(\Delta\omega^2 + \Omega_q^2 - \omega_q^2)^2 n_F(\hbar\Delta\omega)}{\prod_{l=1,2,3}[\Delta\omega_j{}^2 - \omega_l^2]} \tag{24}$$

come from residual calculation.

This is a very general expression, valid for any $\vec{k}$ in the WL plane, which may be evaluated without any problem. Nevertheless, it is more convenient, for devices design purposes, to have a more manageable expression, since in $\Delta\omega_j$ are present $\vec{k}$, $\vec{q}$, and the angle θ between them. We limit calculation to thermalized $\vec{k}=0$ carriers, so integral over in-plane angle ϑ simply results in a 2π factor and q-integral is performed numerically without any stability problem,

$$\tau_{j\to m}^{-1} = \frac{2\alpha c K_\varepsilon\omega_{\mathrm{LO}}^2}{\pi} n_{\mathrm{WL}}|_{(k=0)}\ \mathrm{Im}\int_0^\infty F_{j,m}(q)\{S_{123}(0,q) + S_{312}(0,q) + S_{231}(0,q) - G(0,q)\}d\vartheta\ dq. \tag{25}$$

For low density regimes, ω_+ is the only contributing mode and is very near to ω_{LO}, whereas for high density regimes, all three plasma modes are at play. Nevertheless, it is worth repeating the same calculation above, using this time the static limit of SPP approximation for the dielectric function given by $\varepsilon(q) = (q+\kappa)/q$.

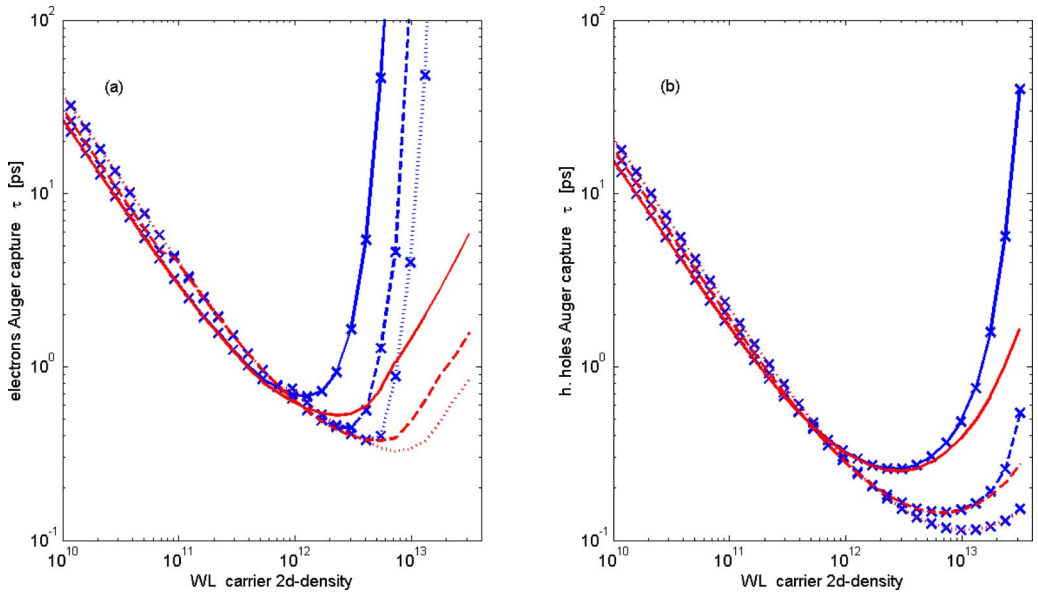

FIG. 1. (Color online) Auger-scattering capture time vs WL carrier density, for electrons (a) and heavy holes (b). Confinement energy has been set to 40 (dotted), 80 (dashed), and 120 meV (solid). *Crossed* lines refer to calculation done keeping Fermi blocking factor (blue lines in the electronic version). For holes the blocking effect is not evident till very high density.

Still considering capture only from states $\vec{k}=0$ in the WL plane and following the path described above for frequency summation, we end with the retarded self-energy,

$$\Sigma_0 = -\pi e^2 K_\varepsilon \ \hbar\omega_{\mathrm{LO}} \ n_{\mathrm{WL}}|_{(k=0)} \sum_q \frac{q}{S(q,\kappa)^{3/2}\left(q+\kappa\frac{\varepsilon_0}{\varepsilon_\infty}\right)^2} \times \frac{1+n_b-n_F}{\frac{\hbar^2 q^2}{2m_e} - \sqrt{S(q,\kappa)}\hbar\omega_{\mathrm{LO}} + E_0 + \mathrm{i}\eta}, \quad (26)$$

where $S(q,\kappa)=\varepsilon_\infty(q+\kappa)/(\varepsilon_\infty q+\varepsilon_0\kappa)$. Without any loss of precision, $\sqrt{S(q,\kappa)}\hbar\omega_{\mathrm{LO}}$ at denominator may be simply approximated by $\hbar\omega_{\mathrm{LO}}$ and summation converted to an integral over $\vec{q}$, carried on remembering that q has to be intended as the norm of the vector $\vec{q}$. We can write q as $\sqrt{q^2}$, being it real and positively defined. In this way, following the method developed in previous works,[16,22] we can extend the integration limit to the negative real axis, dividing the result by two. Then we can extend the integration to the complex plane, adding to the integration path a half-circle at infinity in upper half plane, yielding a vanishing contribution. The only nonvanishing contribution comes from the circular, counterclockwise path around the pole at $q_{\mathrm{pole}} = \sqrt{2m(\hbar\omega_{\mathrm{LO}}-E_0-\mathrm{i}\eta)/\hbar^2}$. The final result, holding for carrier capture by LO-phonon emission, is

$$\tau^{-1}_{\mathrm{phonons}} = \frac{\alpha c\sqrt{2m_e}K_\varepsilon \ \omega_{\mathrm{LO}}}{2} n_{\mathrm{WL}}|_{(k=0)} \times \frac{q^2_{\mathrm{pole}}[1+n_b(\hbar\omega_{\mathrm{LO}})-n_F(\hbar\omega_{\mathrm{LO}}-E_0)]}{S(q_{\mathrm{pole}},\kappa)^{3/2}\left(q_{\mathrm{pole}}+\kappa\frac{\varepsilon_0}{\varepsilon_\infty}\right)^2\sqrt{E_{\mathrm{LO}}-E_0}}. \quad (27)$$

A major difference between Eqs. (22) and (27) consists on the fact that, by using dynamic expression for dielectric function, Fermi band-filling effect is affected by screening; in fact, in Eq. (27) the occupation factor $1+n_b-n_F$ is factorized, whereas in Eq. (22) occupation probability functions appear multiplied by more complicate expressions. Now, a fundamental question clearly appear: below a given value for density N, does static screening lead to correct results?

V. RESULTS AND DISCUSSION

It must be clearly stated that all capture rates calculated in the present formulation already comprise occupation factors, both for WL and QD, and attention must be paid when using them in equation rate systems. Capture times are intended here as the simple inverse of calculated capture rates that comprise the mentioned occupation factors.

In the following, capture times have been evaluated for InAs QD grown on GaAs WL. Electrons and heavy holes effective masses have been set to $m_e=0.064\ m_0$ and $m_{hh}=0.45\ m_0$, being m_0 the free electron mass. As stated in the introduction, no detail on band structure and wave function is explicitly used in the model, except for QD energy confinements with respect to WL, ΔEc for conduction band (CB) and ΔEv for valence band (VB), entering in previous formulae as the parameter E_0. Form factor $F_{j,m}(q)$ has been approximated as in Eq. (9) and set to unity, just to avoid its value to affect the core-results of the model. Temperature has been set to 300 K. Electrons and holes density has been assumed identical, but we stress that in the model they may be given different values as well.

A. Capture via carrier-carrier scattering

In Fig. 1 Auger-scattering capture time $\tau_{j\to j}(N)$, as described by Eq. (17), has been plotted versus WL carrier density, for electrons [Fig. 1(a)] and heavy holes [Fig. 1(b)], for 40, 80, and 120 meV of confinement energy, having aver-

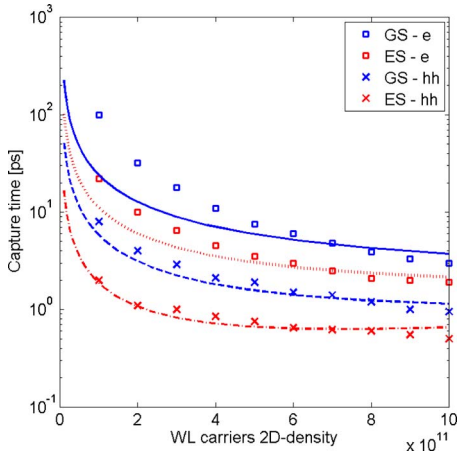

FIG. 2. Capture time for Auger scattering with WL carriers obtained by using the same confinement energies and effective masses values as in Ref. 10, for electrons (e) and holes (hh) GS and ES. Here the superposition integral $I_{i,m}$ has been used as a fitting parameter. GS and ES data points (squares for electrons and crosses for heavy holes) have been extracted from Ref. 10 for comparison (in the electronic version blue symbols and lines refer to GS, red to ES).

aged over a thermally distributed population of WL in-plane $\vec{k}$ states and having summed scattering contributions with both WL electrons and holes. *Crossed* lines refer to calculation carried on keeping in Eq. (17) Fermi distribution n_F; other lines refer to the same calculation obtained discarding (i.e., setting to zero) it. We assume no photons are present in the cavity, so n_B has been always set to zero. In this way it is possible to insulate and separately study screening effects and Fermi band filling. The model well represents the constant decrease in the capture time as WL carrier density increases due to the constant increase in scattering probability. Then, starting around $N=10^{12}$ cm^{-2}, Fermi blocking tends to disfavor further captures (*crossed* lines) but, if we consider lines representing capture times obtained setting to zero n_F (no carriers in the QD), we see that the screening of the interaction causes, as expected, a reduction of capture probability. Fermi blocking is more effective for electrons than for heavy holes, due to the lighter mass of the former, making easier for CB Fermi level to penetrate into the band, with respect to VB.

In order to validate our model, we repeated calculation of the scattering times assisted by WL carriers as in Ref. 10, using $I_{j,m}$ as fitting parameter. In Fig. 2 capture times are plotted versus WL carrier density N. Comparing our results with Fig. 6(a) of Ref. 10, we may notice a good agreement with that more complicate model, especially for intermediate density values. Parameter $I_{j,m}$ has been given values of 0.013, 0.023, 0.04, and 0.13 to match, respectively, electrons ground state (GS) and excited state (ES) capture times (solid and dotted lines) and the corresponding values for heavy holes (dashed and dash-dotted line).

B. Capture via LO-phonon scattering

In Fig. 3 capture time $\tau_{j\to m}(N)$ through screened LO-phonon emission has been plotted, for electrons and heavy holes, as function of carrier density N for several values of confinement energy, as described by Eq. (25) for dynamic

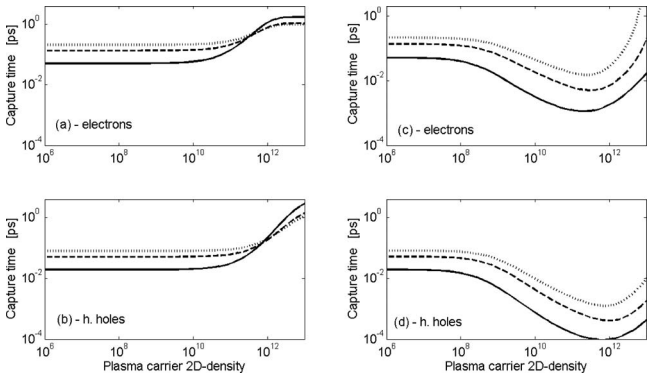

FIG. 3. (Color online) Capture time for LO-phonons emission, using (a) and (b) static screening, whereas in (c) and (d) dynamic SPP screening has been employed, respectively, for electrons and heavy holes, vs WL carrier density. Confinement energy has been set to 20 (dotted), 30 (dashed), and 36 meV (solid).

screening and by Eq. (27) for static screening. In both cases, just to better point out screening effects, n_F and n_B have been temporarily set to zero, but in complete calculation at least n_F must be retained. Solid, dashed, and dotted lines, respectively, refer to 20, 30, and 36 meV confinement energy having assumed unscreened LO-phonon energy E_{LO} to be 37 meV (no capture is possible through single-LO-phonon emission for confinement energy greater than E_{LO}). Effective masses have been given the value as for Auger capture. In Figs. 3(a) and 3(b), the model well shows that static screening slows capture process quite efficiently, but when dynamic aspect of screening is included in the dielectric function [Figs. 3(c) and 3(d)], capture time is significantly reduced both for electrons and heavy holes at intermediate densities, confirming an *antiscreening* effect as pointed out, e.g., in Ref. 23. For high carrier density, antiscreening effect changes to screening and capture time increases as in static approximation.

As far as obtained values for capture time are concerned, we remind that the superposition integral $I_{j,m}$ has been given unity value, in order not to specify anything about it. True capture times may be given by values evaluated by the present model (and shown in the plots), divided by $I_{j,m}$, in whatever way it is calculated. Better precision may be obtained using Eq. (9) instead of Eq. (10) in the equations, but this task is beyond the scope of this paper.

VI. CONCLUSION

In conclusion, we studied carrier capture from WL to confined states of QD, in dynamic SPP approximation of RPA dielectric function, obtaining for the first time explicit expressions not available in literature in this form at the degree of approximation of the present formulation. The present formulation goes beyond the Fermi golden rule, including population effects. Analytical integration over energy in $[0,\infty]$ interval by means of residual theorem avoids a very time consuming numerical integration and yields practical formulations, ready to be employed in device simulation codes.

Present model may easily offer better precision using Eq. (9) instead of Eq. (10), provided form factor has been evalu-

ated. The model effectively describes the initial capture time reduction for increasing carrier density through Auger scattering mechanism, due to increased scattering probability in good agreement both with more rigorous theoretical models[10] and measurement results,[8] accounting also for dynamic aspect of the screening. As far as capture through LO-phonon emission is concerned, we obtained an explicit expression describing the antiscreening effect at intermediate density, followed by a standard screening effect when carrier density becomes very high, in a way not clearly described up to now. At intermediate densities both capture mechanisms play an important role and must be taken into account, but at least at high carrier density the main capture mechanism for electrons is confirmed to be the Auger scattering (see, e.g., Ref. 7 for an experimental review). For low carrier density, heavy holes may be efficiently captured in QDs through LO-phonon emission, giving rise to different carrier density for electrons and holes in QDs, which a rate-equation model should keep into account.

ACKNOWLEDGMENTS

The research leading to these results has received funding from the European Community's Seventh Framework Programme (FP7/2007-2013) under Grant Agreement No. 224338 (FAST-DOT project).

[1]P. Bhattacharya, K. K. Kamath, J. Singh, D. Koltzkin, J. Phillips, H.-T. Jiang, N. Chervela, T. B. Norris, T. Sosnowski, J. Laskar, and M. R. Murty, IEEE Trans. Electron Devices **46**, 871 (1999).
[2]H. Johnson, V. Nguyen, and A. Bower, J. Appl. Phys. **92**, 4653 (2002).
[3]A. Markus, J. Chen, O. G. L. Provost, C. Parathoen, and A. Fiore, IEEE J. Sel. Top. Quantum Electron. **9**, 1308 (2003).
[4]M. Sugawara, K. Mukai, Y. Nakata, H. Ishikawa, and A. Sakamoto, Phys. Rev. B **61**, 7595 (2000).
[5]H. Huang and D. Deppe, IEEE J. Quantum Electron. **37**, 691 (2001).
[6]J. Shah, *Ultrafast Spectroscopy of Semiconductors and Semiconductor Nanostructures* (Springer, Berlin, 1996).
[7]P. Borri, S. Schneider, W. Langbein, and D. Bimberg, J. Opt. A, Pure Appl. Opt. **8**, S33 (2006).
[8]T. Piwonski, I. O'Driscoll, J. Houlihan, G. Huyet, and R. J. Manning, Appl. Phys. Lett. **90**, 122108 (2007).
[9]I. O'Driscoll, T. Piwonski, C.-F. Schleussner, J. Houlihan, G. Huyet, and R. J. Manning, Appl. Phys. Lett. **91**, 071111 (2007).
[10]T. R. Nielsen, P. Gartner, and F. Jannke, Phys. Rev. B **69**, 235314 (2004).
[11]M. Sugawara, N. Hatori, H. Ebe, M. Ishida, Y. Arakawa, T. Akiyama, K. Otsubo, and Y. Nakata, J. Appl. Phys. **97**, 043523 (2005).
[12]G. D. Mahan, *Many Particle Physics* (Plenum, New York, 1981).
[13]H. Haug and A.-P. Jauho, *Quantum Kinetics in Transport and Optics of Semiconductors* (Springer-Verlag, Heidelberg, 1996).
[14]P. Sotirelis and K. Hess, Phys. Rev. B **49**, 7543 (1994) and references herein.
[15]P. Sotirelis, P. von Allmen, and K. Hess, Phys. Rev. B **47**, 12744 (1993).
[16]D. Campi, G. Colì, and M. Vallone, Phys. Rev. B **57**, 4681 (1998).
[17]K. Lüdge, M. J. P. Bormann, E. Malić, P. Hövel, and D. Matthias Kuntz, Phys. Rev. B **78**, 035316 (2008).
[18]D. Reschner, E. Gehring, and O. Hess, IEEE J. Quantum Electron. **45**, 21 (2009).
[19]R. H. Lyddane, R. G. Sachs, and E. Teller, Phys. Rev. B **59**, 673 (1941).
[20]T. Y. Wang and G. B. Stringfellow, J. Appl. Phys. **67**, 344 (1990).
[21]H. Haug and S. W. Koch, *Quantum Theory of the Electronic Properties of Semiconductors* (World Scientific, Singapore, 1990).
[22]M. Vallone, D. Campi, and C. Cacciatore, J. Appl. Phys. **87**, 2947 (2000).
[23]J.-Z. Zhang and I. Galbraith, Appl. Phys. Lett. **89**, 153119 (2006).